

Comparison of a large-scale inertia-gravity wave as seen in the ECMWF analyses and from radiosondes

R. Plougonven¹ and H. Teitelbaum²

Received 9 May 2003; revised 1 August 2003; accepted 7 August 2003; published 25 September 2003.

[1] The location, characteristics and evolution of a large-scale inertia-gravity wave that occurred in the lower stratosphere over the North of the British Isles on February 6, 1997, are studied. Numerous high-resolution radiosondes were available at that time and in that region as part of the FASTEX database. They reveal an intense, large-scale inertia-gravity wave (IGW), propagating upwards above the tropopause. Maps of the divergence of the horizontal wind, on isentropic surfaces, were obtained from the ECMWF analyses, and showed a clear pattern of alternating bands of convergence and divergence, at the lower stratospheric heights, in the same geographical region and starting at the same time. The comparison of the characteristics of this IGW in the analyses and in the observations suggests that the ECMWF analyses can be used for qualitative indications regarding the locations most favorable to large-scale IGW generation and the corresponding orientation of the waves. *INDEX*

TERMS: 3329 Meteorology and Atmospheric Dynamics: Mesoscale meteorology; 3337 Meteorology and Atmospheric Dynamics: Numerical modeling and data assimilation; 3384 Meteorology and Atmospheric Dynamics: Waves and tides. **Citation:** Plougonven, R., and H. Teitelbaum, Comparison of a large-scale inertia-gravity wave as seen in the ECMWF analyses and from radiosondes, *Geophys. Res. Lett.*, 30(18), 1954, doi:10.1029/2003GL017716, 2003.

1. Introduction

[2] Analyses of operational centers such as the European Center for Medium-Range Weather Forecasts (ECMWF) are commonly used in observational studies to describe the synoptic-scale situation within which smaller-scale phenomena are investigated from measurements. For instance, recent studies used these analyses, along with observations, to identify regions where generation of IGW through geostrophic adjustment was likely [Hertzog *et al.*, 2001], or to support results obtained from soundings for the location and orientation of IGW [Moldovan *et al.*, 2002; Plougonven *et al.*, 2003]. The agreement between the observations and the analyses was encouraging, and it is legitimate to ask how reliable is the information on IGWs obtained from the ECMWF analyses (location and time of appearance of the waves, their orientation, extent, wavelengths, and evolution).

¹ASP/MMM, National Center for Atmospheric Research, Boulder, Colorado, USA.

²Laboratoire de Météorologie Dynamique, ENS, Paris, France.

[3] The resolution of the general circulation models (GCM) has become such that their dynamical cores are now intrinsically able to simulate realistic large-scale IGWs. In fact, in the last decade, GCMs have been increasingly used to study IGWs, e.g. for the detailed investigation of their generation by the midlatitude tropospheric jet [O'Sullivan and Dunkerton, 1995], or for global statistics of the IGW field [Sato *et al.*, 1999]. Such studies support that GCMs are able to describe these kinds of waves.

[4] The aim of this paper is to compare the location, characteristics and evolution of a large-scale IGW from the ECMWF analyses with observations. We have chosen to focus on a wave which extended over a broad region centered on Scotland, on February 5 and 6, 1997, because the wave pattern is clear in the ECMWF analysis and the available soundings are numerous. Section 2 describes the synoptic situation, the generation and the evolution of the IGW in the analyses. Section 3 presents the characteristics and evolution of the IGW that can be obtained from the soundings. The comparison of the ECMWF analyses with the observations is given in Section 4. Possible uses of ECMWF analyses in studies on IGWs are discussed in Section 5.

2. The ECMWF Analyses

[5] The synoptic situation from February 5, 12GMT, to February 6, 18GMT, at upper-tropospheric levels, consists of a ridge in the geopotential moving eastwards over the British Isles (see Figure 1), with a jet maximum upstream of the ridge. Uccellini and Koch [1987] have put forward this configuration as particularly favorable to the generation of large-scale IGWs in the anticyclonic side of the exit region of the velocity maximum.

[6] In maps of divergence of the horizontal wind for the lower stratosphere (typically 10–15 km), distinct patterns of alternating bands of convergence and divergence are often seen. They are interpreted as the signature of an IGW. In the present case we display such maps for times corresponding to the generation of the wave in Figure 2. The wave appears on February 5, between 12.00GMT and 18.00GMT (Figures 2a and 2b). The wave pattern is then intense and very distinct until February 7, 00.00GMT. During that time interval, it progressively moves eastward and northward over to Scandinavia.

[7] From these maps we deduce that the wave-vectors are essentially zonal (Figures 2b and 2c) and that the horizontal wavelength lies between 400 and 600 km. The examination of these maps at different levels show that the vertical wavelength lies between 6 and 10 km, and that the phase surfaces tilt westward with height. Comparing maps that are 6 hours apart, it appears that the wave is stationary relative to the ground.

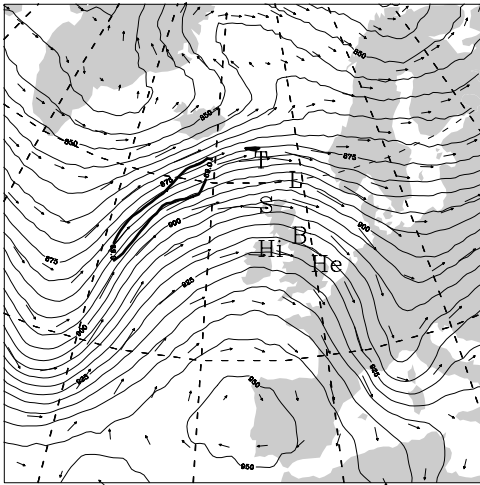


Figure 1. Map of the geopotential and wind at log-pressure height $Z = 8$ km (approximately 300hPa), on February 6, 00GMT. The thick line indicates the region of maximum wind (69 ms^{-1} isotach). The letters indicate the locations of stations from which radiosoundings were launched (c.f. Section 3).

[8] For a more detailed analysis of the wave structure, the wind and potential temperature were split into a background and a perturbation. The perturbation was obtained by subtracting fields that had been smoothed horizontally from the initial fields. For a linear inertia-gravity wave with a horizontal wavevector oriented zonally ($k > 0$, $l = 0$), the wave variables can be expressed as [cf. Holton, 1992, Section 7.5]:

$$(u', v', \theta', p') = \text{Re} \left[(\hat{u}, \hat{v}, \hat{\theta}, \hat{p}) e^{i(kx + mz - \omega t)} \right].$$

[9] Assuming for simplicity $\hat{p} = 1$, the following polarization relations are obtained from the linearized equations:

$$\hat{u} = \frac{\omega k}{\omega^2 - f^2}, \quad \hat{v} = \frac{-ifk}{\omega^2 - f^2}, \quad \hat{\theta} = i \frac{m\bar{\theta}}{g}, \quad (1)$$

where $\bar{\theta}$ is the background stratification. The phase relationship between u' and v' (Figures 2e and 2f) implies that $\omega < 0$, which is consistent with the westward propagation relative to the mean flow. From Figures 2d and 2f, we deduce that $m > 0$, which is consistent with upward propagation of the wave energy and the westward tilt of the phase surfaces. Finally, from the polarization relations, we expect the divergence and θ' to be in opposition, and this is verified (Figures 2c and 2d).

[10] Hodographs made from horizontal profiles of u' and v' , along a parallel and at a given height, show ellipses oriented essentially in the zonal direction, with aspect ratios of 0.5–0.7, suggesting that the wave has an intrinsic frequency of 1.4 – $2f$. This is consistent with the horizontal and vertical wavelengths and with the dispersion relation.

[11] We have used, to describe the synoptic situation and some wave characteristics, analyses from the ECMWF. It is unclear a priori whether the wave is produced by the

model's dynamics or by the assimilation procedure. In order to answer this question, maps of divergence as those displayed in Figure 2 were obtained from 6 hour and 12 hour forecasts; they are hardly distinguishable from the ones obtained using the analyses. Even for 24h and 36h forecasts, the wave is present and very similar (N. Wedi, personal communication). Now, as the wave is not present in the analysis from which the model starts in order to produce these forecasts, this strongly suggests that the wave is produced by the model's dynamics, and not by the assimilation procedure.

3. Generation and Evolution of the Wave According to the Radiosondes

[12] Radiosondes launched from stations in that region were investigated to see if the observations indeed revealed important inertia-gravity wave activity at that time. Clear

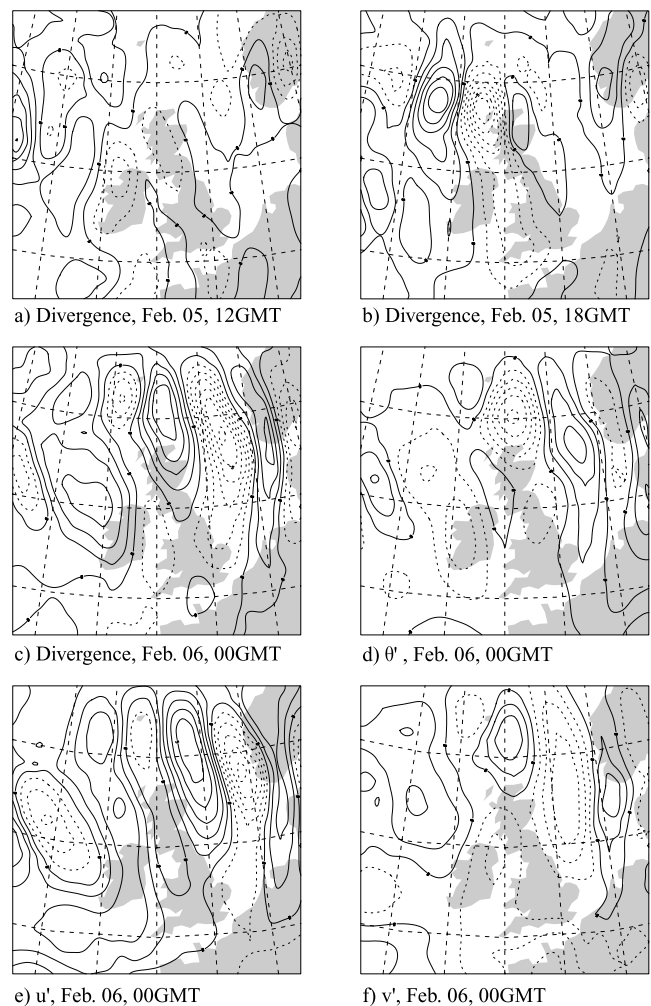


Figure 2. (a–c): Maps of the divergence of the horizontal wind on isobaric surface 158hPa, latitudes and longitudes are plotted every 5 degrees. (d–f): Maps of the perturbation of the potential temperature, zonal velocity and meridional velocity for February 6, 00GMT, on the same surface (contour intervals are 1K for the potential temperature and 1 ms^{-1} for the velocities).

and intense IGW activity was found in 6 stations and their locations are indicated by letters in Figure 1: Hillsborough (Hi), Lerwick (L), Stornoway (S), Boulmer (B), and Hemsby (He) from the United Kingdom, and Thorshavn (T) from the Faroe Islands (Denmark). There were up to eight soundings per day for those stations; in a great number of these soundings, starting from February 5, 12GMT, to February 6, around 18GMT, intense IGW activity was distinctly observed in the lower stratosphere (wind disturbances typically $6\text{--}8\text{ ms}^{-1}$). In soundings from stations more to the South–West (Wales, Cornwall, South–West Ireland) or from Iceland, comparable clear and intense IGW activity was not observed. This sets bounds to the horizontal extent of the wave.

[13] In order to estimate the wave’s characteristics, the wind profiles were separated into a background and a perturbation using a non-recursive filter described in *Scavuzzo et al.* [1998], with a window intended to eliminate large and small scale perturbations. The vertical wavelength was obtained from the vertical profiles of the latter, and the intrinsic frequency from the aspect ratio of the corresponding hodograph (e.g. Figure 3).

[14] The hodographs suggest that an intense IGW is generated at the level of the jet over the North of Ireland, starting from February 5 at 12GMT. A wave propagating downward in the troposphere (cyclonic rotation in the hodograph) and a wave propagating upward in the stratosphere (anticyclonic rotation) can be seen in the soundings of Hillsborough (Figure 3a) and Stornoway (not shown). This wave is then found in soundings more to the East and North. In the morning of February 6, it has its greatest horizontal extent from Thorshavn (generation at the level of the jet is here again evident, see Figure 3d) to Hemsby. After February 6, 12GMT, the wave is found in fewer soundings.

[15] The characteristics of the IGW observed in 18 soundings are listed in Table 1. They generally correspond to a wave of 2–3 km vertical wavelength, present in the lower stratosphere (10–15 km) until around 12GMT on February 6, higher above afterwards (12–20 km) consistent with a vertical propagation. The orientation of the wave-vectors, as deduced from the hodographs, ranges from a Northwest–Southeast orientation (Figures 3a and 3c) to a Southwest–Northeast orientation at late times. The aspect ratios are typically between 0.3 and 0.6, but for a few soundings, they may be higher, suggesting a lower frequency. The horizontal wavelengths estimated using the linear dispersion relationship range typically from 100 km to 400 km.

[16] In the soundings launched from Lerwick, Stornoway and Hillsborough in the morning of February 6th, the vertical displacement of the phase over three hours was found to be of 200–400m upward. This suggests that, for a wavevector pointing eastwards, the intrinsic frequency of the wave is negative (westward propagation). This is also indicated by the phase relationships between the perturbations of the wind and of potential temperature.

[17] The characteristics of the waves are not uniform, but they are comparable in a considerable number of soundings, especially in the earliest ones. As time advances, the variability of the wave characteristics increases; our interpretation is that the wave is generated on a large-scale, but

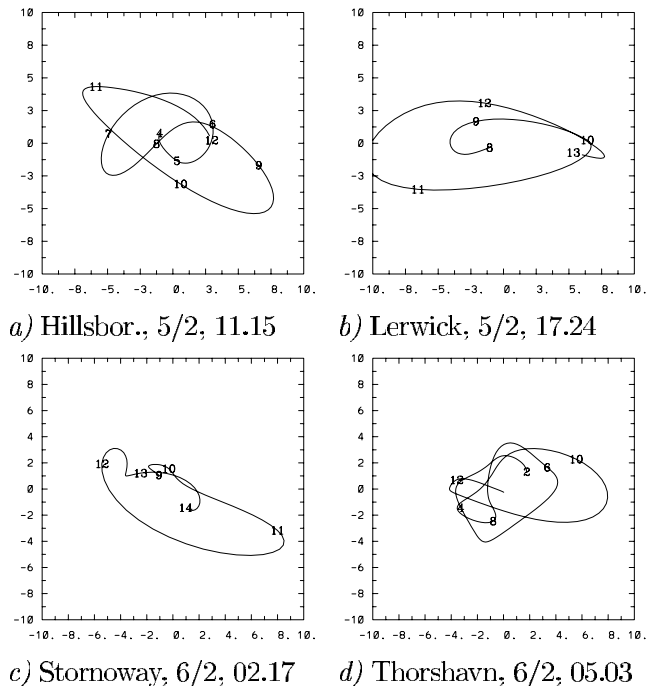


Figure 3. Hodographs of four of the radiosoundings. The numbers indicate altitudes in km.

that its subsequent evolution in different regions of the flow may vary considerably.

4. Comparison of the Analyses With the Observations

[18] In this example, observations confirm the existence of an intense IGW at the location and time indicated by the ECMWF analyses: generation in the afternoon of February 5 North of Ireland, propagation to the East and North, maximum extension on February 6, between 00GMT and 12GMT. The orientation (wavevector essentially zonal and against the flow) and even the amplitude of the waves are also comparable.

[19] However the agreement between the observations and the analyses does not extend to the wavelength and the evolution of the wave. The resolution of the ECMWF is too coarse, particularly in the vertical, and the wavelengths are overestimated by a factor 2 or 3 (the model is run with a resolution of about 50 km horizontally, 15 min. in time, and 60 levels in the vertical up to 1hPa; the analyses are retrieved with only 15 pressure levels in the vertical, up to 10hPa, and every 6 hours). The wave disappears from the soundings earlier than in the analyses, and the characteristics of the wave in the soundings varies much more, at late times, than what can be described by the ECMWF. The IGW and its evolution are evidently more complex in reality (e.g., encounter of critical levels, effect of differential advection) than what can be described by the ECMWF.

5. Discussion

[20] This detailed comparison suggests that analyses of the ECMWF can be useful for indications on the time and location of generation of large-scale IGWs and on

Table 1. Characteristics of the Waves for Eighteen Radiosoundings in Which an Inertia-gravity Wave was Clearly Present in the Lower Stratosphere Between February 5, 12.00GMT, and February 6, 24.00GMT

Location & Time	Height	Filtering Band	λ_z	R	λ_h	u_{max}
Hi, 5/2, 11.15	8.5–12.5 km	1.5–5 km	2.7 km	0.33	180 km	8 ms⁻¹
L, 5/2, 17.24	8–13 km	1–5 km	2.7 km	0.40	200 km	10 ms⁻¹
Hi, 5/2, 20.15	9.5–15 km	1.5–5 km	2.2 km	0.4–0.7	180–400km	4 ms ⁻¹
S, 5/2, 23.19	10–13 km	1–5 km	2.4 km	.25	100 km	8 ms ⁻¹
B, 5/2, 23.17	10–13 km	1–5 km	1.7 km	~1	–	6 ms ⁻¹
L, 6/2, 02.16	10–12 km	1–5 km	1.8 km	0.45	150 km	6 ms ⁻¹
Hi, 6/2, 02.16	10–15 km	1.5–5 km	2.6 km	0.67	410 km	4 ms ⁻¹
S, 6/2, 02.17	10–13 km	1–5 km	2 km	0.33	110 km	7 ms⁻¹
T, 6/2, 05.03	9–12 km	1–5 km	2.8 km	0.4	210 km	6 ms⁻¹
Hi, 6/2, 05.15	12–14 km	1–5 km	1.5 km	0.56	220 km	4 ms ⁻¹
L, 6/2, 05.16	10–14 km	1–5 km	2.8 km	0.5	280 km	8 ms ⁻¹
S, 6/2, 05.17	10–15 km	2–6 km	4.2 km	0.2	150 km	8 ms ⁻¹
He, 6/2, 05.16	10–19 km	1.5–5 km	2.2 km	0.55–0.7	260–400 km	4 ms ⁻¹
L, 6/2, 08.16	10–15 km	1–5 km	3.1 km	0.38	220 km	6 ms ⁻¹
S, 6/2, 08.19	11–14.5 km	1–5 km	1.5 km	0.45–0.65	140–250 km	4 ms ⁻¹
S, 6/2, 08.19	14.5–18 km	1–5 km	2.8 km	0.8	720 km	5 ms ⁻¹
S, 6/2, 11.19	12–17 km	1–5 km	2 km	0.4–0.75	170–450 km	7 ms ⁻¹
Hi 6/2, 14.15	13–17 km	1–5 km	2.2 km	0.4	175 km	7 ms ⁻¹
B, 6/2, 17.16	14–20 km	1–5 km	3.1 km	0.5	294 km	6 ms ⁻¹

Successive columns show the time and location of the soundings, the heights at which the waves were observed, the filtering band used to obtain the wave characteristics, the vertical wavelength, the aspect ratio of the ellipse seen in the hodograph, the estimated horizontal wavelength and the maximum horizontal velocity. The lines corresponding to the hodographs displayed in Figure 3 are written in bold.

their orientation. On the other hand, it should not be used for quantitative indications on their wavelengths or their evolution.

[21] Comparisons of the analyses and forecasts show that the wave is likely produced by the model's dynamics, not by the assimilation procedure. Our interpretation is that the model's resolution allows it to describe the forcing by the large-scale flow of a region of imbalance (in the jet exit region, ageostrophic winds of more than 30 m/s are present, corresponding to Lagrangian Rossby numbers higher than 0.45, and cross-stream Lagrangian Rossby [Koch and Dorian, 1988] numbers higher than 0.3); this imbalance adjusts and excites inertia-gravity waves, but the resolution of the model is not fine enough for a quantitatively accurate description of these IGWs and of their evolution. Hence the time and location of the wave generation is right, but the waves' characteristics and evolution are not. Indeed, simulations made at various resolutions by O'Sullivan and Dunkerton [1995] suggested that, at low resolutions, the intensity and wavelength of the simulated IGWs were not reliable, but that the location of their generation and their orientation were consistent with higher resolution simulations.

[22] Hence, we suggest that maps of the divergence of the horizontal wind in the lower stratosphere can be used, for example, to provide guidance concerning which days and locations of a large dataset it is worthwhile to investigate in detail for studies of inertia-gravity wave generation by the jet. A better understanding of the mechanism responsible for the generation of the waves is however necessary to assess more generally how much ECMWF analyses can be relied upon for these purposes.

[23] **Acknowledgments.** The authors are grateful to Nils Wedi for additional comparisons of the ECMWF analyses and forecasts. R.P. wishes to thank Joe Tribbia, Luc Fillion and Byron Boville for instructive and stimulating discussions, and Rich Rotunno for his helpful comments on the manuscript.

References

- Holton, J. R., *Introduction to dynamic meteorology*, 3rd edn, Academic, San Diego, CA, 1992.
- Hertzog, A., C. Souprayen, and A. Hauchecorne, Observation and backward trajectory of an inertia-gravity wave in the lower stratosphere, *Ann. Geophys.*, *19*, 1141–1155, 2001.
- Koch, S. E., and P. B. Dorian, A mesoscale gravity wave event observed during CCOPE. Part III: Wave environment and possible source mechanisms, *Mon. Wea. Rev.*, *116*, 2570–2591, 1988.
- Moldovan, H., F. Lott, and H. Teitelbaum, Wave breaking and critical levels for propagating inertial gravity waves in the lower stratosphere, *Q. J. R. Meteorol. Soc.*, *128*, 713–732, 2002.
- O'Sullivan, D., and T. Dunkerton, Generation of inertia-gravity waves in a simulated life cycle of baroclinic instability, *J. Atmos. Sci.*, *52*, 3695–3716, 1995.
- Plougonven, R., H. Teitelbaum, and V. Zeitlin, Inertia-gravity wave generation by the tropospheric mid-latitude jet as given by the FASTEX radiosoundings, *J. Geophys. Res.*, doi:10.1029/2003JD003535, in press, 2003.
- Sato, K., T. Kumakura, and M. Takahashi, Gravity waves appearing in a high-resolution GCM simulation, *J. Atmos. Sci.*, *56*, 1005–1018, 1999.
- Scavuzzo, C., M. Lamfri, H. Teitelbaum, and F. Lott, A study of the low-frequency inertia-gravity waves observed during the Pyrénées Experiment, *J. Geophys. Res.*, *103*, 1747–1758, 1998.
- Uccellini, L., and S. Koch, The synoptic setting and possible energy sources for mesoscale wave disturbances, *Mon. Wea. Rev.*, *115*, 721–729, 1987.

R. Plougonven, MMM/ASP, National Center for Atmospheric Research, P.O. Box 3000, Boulder, CO 80307-3000, USA. (riwal.plougonven@polytechnique.org)

H. Teitelbaum, Laboratoire de Météorologie Dynamique Ecole Normale Supérieure 24 rue Lhomond, 75231 Paris Cedex 05, France. (teitel@lmd.ens.fr)